Binucleating N_6 24- and 26-Membered Macrocyclic Ligands. Part 2.[1] Transition-metal Homo- and Hetero-binuclear Complexes: *X*-Ray Crystallographic Structure Determination of a Lead–Manganese Heterobinuclear Complex†

Jane Nelson * **and Brian P. Murphy**
The Open University, Milton Keynes MK7 6AA
Michael G. B. Drew * **and Paul C. Yates**
The University, Whiteknights, Reading RG6 2AD
S. Martin Nelson
Queen's University, Belfast BT9 5AC

Template condensation products of 1,5-diaminopentane and 1,6-diaminohexane with 2,6-diacetylpyridine on $Pb(NCS)_2$ have been transmetallated with Co^{II} and Cu^{II} to yield homobinuclear complexes of the 24- and 26-membered macrocycles, L^1 and L^2 respectively. In the dicobalt(II) complex of the smaller macrocycle, L^1, a thermally populated spin equilibrium exists lying well to the low-spin side at 93 K. E.s.r. spectra indicate the complex has an equatorially compressed tetragonal geometry. The dicobalt(II) complex of the larger macrocycle, L^2, is effectively high-spin, down to 93 K. Dicopper(II) complexes of L^1 display a weak antiferromagnetic interaction, absent in analogous complexes of L^2. Heterobinuclear complexes $[PbML^1(NCS)_2(MeCN)_2][ClO_4]_2$ of the 24-membered macrocycle have been prepared for M = Ni^{II} and Fe^{II}, as confirmed by fast-atom bombardment (f.a.b.) mass spectra. An *X*-ray crystallographic structure determination on the heterobinuclear complex $PbMnL^1(NCS)_4$ reveals a Pb–Mn distance of 4.857(2) Å and confirms that the metal centres are bridged by two 1,3-μ –NCS– bridges, as inferred from i.r. spectroscopy for the other thiocyanato complexes studied. However, the *X*-ray structure shows that in this case the thiocyanate bridges present both S-donors to Pb and both N-donors to Mn.

In Part 1[1] we showed that 1,5-diaminopentane and 1,6-diaminohexane undergo template Schiff-base condensation with 2,6-diacetylpyridine on $Pb(NCS)_2$ to form 24- and 26-membered macrocycles, L^1 and L^2 respectively.

X-Ray crystallographic structure determination[1] shows that in $Pb_2L^1(NCS)_4$ the macrocycle adopts an approximately face-to-face conformation for the pyridylmethylimino units; the two PbN_3 moieties intersect each other at an angle of 47.9°. The pentane linkages between the pyridylmethylimino units are planar and intersect the two PbN_3 moieties at angles of 65.8 and 66.3°. Presumably this conformation is required to accommodate the single-atom >NCS thiocyanate bridge connecting the two lead ions which are 4.347(1) Å apart. The present work describes the transmetallation products of $Pb_2L^1(NCS)_4$ and $Pb_2L^2(NCS)_4$ with first transition-series ions Mn^{II}, Fe^{II}, Co^{II}, Ni^{II}, and Cu^{II}. The mode of co-ordination of the NCS bridging ligand, where retained, is diagnostic of the separation of the metal centres in the binuclear transmetallation product. The, by now, well established infrared spectroscopic criterion[2] that $\nu_{asym}(NCS)$ $< 2\,000$ cm^{-1} characterises single-atom >NCS bridging, while $\nu_{asym}(NCS)$ $\geqslant 2\,100$ cm^{-1} indicates the more usual three-atom –NCS– bridge, can serve to establish, at least qualitatively, the distance between the metal centres.

Binuclear complexes of relatively restricting macrocyclic ligands such as L^1 are of interest because the metal ions may be forced into unusual bonding situations in the small macrocyclic cavity producing unusual and perhaps even useful properties. Heterobinuclear complexes are of particular interest in this respect; the possibility of enhancing the reactivity of small substrate molecules which bridge the two different metal centres has attracted much attention.

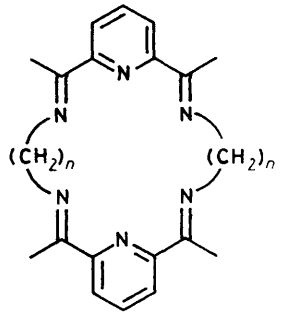

L^1 ; $n = 5$
L^2 ; $n = 6$

Results and Discussion

Homobinuclear Complexes.—Treatment of the dilead complexes $Pb_2L(X)_4$ (L = L^1 or L^2; X = ClO_4^- or NCS^-) with an excess of the appropriate transition-metal salt gives dicopper(II) and dicobalt(II) complexes, as characterised in Table 1. The dicopper(II) tetraperchlorate derivatives are 1:4 electrolytes in acetonitrile solution as shown by conductivity measurements,[3] although splitting of ν_3 and ν_4 ClO_4^- i.r. absorptions indicates co-ordination of the counter ion in the solid state. The bis-thiocyanato complexes $[M_2L(NCS)_2]X_2$ are at least 1:2 electrolytes in acetonitrile solution. Their solid-state i.r. spectra show a $\nu_{asym}(NCS)$ absorption in the range typical of 1,3-μ –NCS– bridging. This absorption shows a splitting, sometimes

† *Supplementary data available:* see Instructions for Authors, *J. Chem. Soc., Dalton Trans.*, 1988, Issue 1, p. xvii—xx.

Non-S.I. units employed: cal = 4.184 J, G = 10^{-4} T, B.M. = 9.27×10^{-24} J T^{-1}, dyn = 10^{-5} N.

Table 1. Analytical, conductance, and i.r. (cm^{-1}) spectral data

Complex	Analysis (%) Found N	C	H	Calc. N	C	H	Λ^a/S cm^2 mol^{-1}	I.r. ν_{asym}(NCS)	ν(C=N)	$\nu_3(ClO_4^-)$	$\nu_4(ClO_4^-)$
$[Co_2L^1(NCS)_2(MeCN)_2][ClO_4]_2\cdot 2H_2O$	13.7	40.8	4.6	13.9	40.5	4.4	270	2 128s, 2 110s, 2 070 sh,	1 628mw	1 140 (sh), 1 100s, 1 055s	640ms, 628ms
$[Co_2L^2(NCS)_2(MeCN)_2][ClO_4]_2\cdot 2H_2O$	13.5	41.6	5.2	13.5	41.7	5.1	3312	2 120 (sh), 2 100s	1 625m	1 110s,br	630ms, 625ms
$[Co_2L^1(NCS)_2(MeCN)_2][BPh_4]_2$	9.7	68.5	6.1	9.9	69.7	5.6	339	2 130 (sh), 2 122s	1 622w		
$[Co_2L^2(NCS)_2(MeCN)_2][BPh_4]_2$	9.7	70.0	5.7	9.2	70.0	6.1	350	2 095s	1 622m		
$[Cu_2L^1(NCS)_2][ClO_4]_2\cdot H_2O$	12.3	39.3	4.3	12.2	39.2	4.4	326	2 118s	1 625m	1 090s,br	625ms
$[Cu_2L^2(NCS)_2][ClO_4]_2\cdot 2H_2O$	11.5	39.8	4.6	11.6	39.8	4.8	338	2 104s, 2 080 (sh)	1 622m	1 090s,br	625ms
$[Cu_2L^1(NCS)_2][BPh_4]_2\cdot H_2O$	8.4	68.8	5.8	8.3	69.0	5.8	272	2 120s, 2 100 (sh)	1 616m		
$[Cu_2L^2(NCS)_2][BPh_4]_2$	8.0	69.7	6.1	8.2	70.0	6.0	260	2 120s, 2 095 (sh)	1 617m		
$PbMnL^1(NCS)_4$	14.5	40.5	4.3	14.7	40.3	4.0	*b*	2 090s, 2 062s, 2 022s	1 635m,br		
$[PbMnL^1(NCS)_2][ClO_4]_2$	11.2	33.9	3.7	10.8	34.8	3.7	*b*	2 090s, 2 065s, 1 965s	1 635m, 1 622m	1 090s,br	635ms, 625ms
$[PbFeL^1(NCS)_2(MeCN)_2][ClO_4]_2$	12.0	36.9	4.0	12.5	36.4	4.0	*b*	2 122 (sh), 2 102s, 2 070s	1 638mw, 1 622mw	1 090s,br	623ms
$[PbNiL^1(NCS)_2(MeCN)_2][ClO_4]_2$	12.2	35.9	3.9	12.5	36.4	3.9	*b*	2 130 (sh), 2 118s, 2 095s	1 635m, 1 625m	1 095s,br	625ms
$[Cu_2L^1(H_2O)_4][ClO_4]_4$	8.2	31.9	4.3	8.0	32.0	4.4	424		1 618m	1 140vs, 1 108vs, 1 085vs	635ms, 628ms, 622ms
$[Cu_2L^2(dmf)_2(H_2O)_2][ClO_4]_4$	9.6	36.2	5.0	9.4	36.2	5.1	540		1 621m	1 125vs, 1 085vs, 1 038vs	626ms, 622ms, 618ms

[a] 1×10^{-3} mol dm^{-3} solution in MeCN. [b] Insoluble.

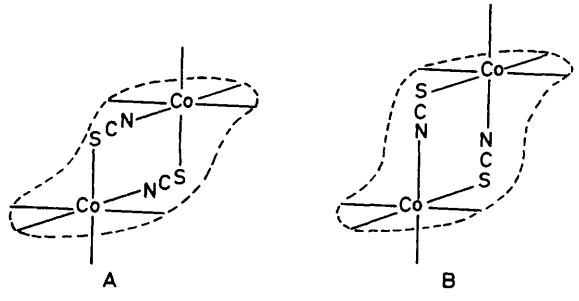

Figure 1. Equatorial–axial thiocyanate bridges in $[Co_2L(NCS)_2(MeCN)_2]^{2+}$

well but sometimes only poorly resolved, suggesting a low-symmetry environment for thiocyanate. In the acetonitrile solvates, $[Co_2L(NCS)_2]X_2\cdot 2MeCN$, i.r. spectra show that acetonitrile is co-ordinated, providing evidence for six-co-ordination of Co^{II}. When thiocyanate co-ordinates *via* sulphur, a M–S–C angle of *ca.* 90° is normally observed, whereas when N is the donor the M–N–C geometry is close to linear. These geometric preferences can be accommodated in the 1,3-μ bridge if one end is disposed axially towards the first metal ion and the other equatorially towards the second metal ion. Figure 1 illustrates two forms of this axial–equatorial bridge.

A further feature noticeable in the i.r. spectrum of $[Co_2L^1(NCS)_2(MeCN)_2]X_2$ complexes is the weakness of the macrocyclic ν(C=N) imino absorption at *ca.* 1 620 cm^{-1}. This absorption is normally absent or strongly reduced in intensity[4] in trimethine complexes of low-spin Fe^{II} or Co^{II}. The intermediate intensity observed in this case suggests the operation of a $^4T_{1g} \rightarrow {}^2E_g$ spin equilibrium, with appreciable population of both states at room temperature. Variable-temperature magnetic susceptibility measurements (Table 2 and Figure 2) support this interpretation; these dicobalt(II) complexes show abnormally low room-temperature magnetic moments, which reduce further on cooling to 93 K. At this temperature, it appears that the equilibrium lies well to the low-spin side. The cobalt(II) complexes of L^2, on the other hand, display a medium i.r. ν(C=N) imino stretching absorption around 1 620 cm^{-1} and a normal high-spin room-temperature magnetic moment, which is only slightly reduced on cooling to 93 K. It appears that the ligand field is noticeably smaller in the case of this larger macrocycle, an observation which is at first sight surprising, because the donor set is identical in the two complexes.

At 89 K, the dicobalt complexes of L^1 have the simple e.s.r. spectrum expected for spin-paired cobalt(II). Thus, a polycrystalline sample of $[Co_2L^1(NCS)_2(MeCN)_2][BPh_4]_2$ shows a $g \approx 2$ signal with eight broad components in the parallel band. The signal was sharper when $[Co_2L^1(NCS)_2]^{2+}$ was run as a

Table 2. Magnetic, e.s.r., and electronic spectral data

Complex	Colour	$\mu_{eff.}$/B.M. 393 K	$\mu_{eff.}$/B.M. 93 K	E.s.r. data[a] $g_\perp$	$g_\parallel$	$A_\parallel$/G	Electronic spectra[b] MeCN solution	Nujol mull
$[Co_2L^1(NCS)_2(MeCN)_2][ClO_4]_2\cdot 2H_2O$	Dark brown	3.20	2.17	2.27[c]	2.04[c]	97[c]	22 000 (sh) (*ca.* 2 600), 18 000 (2 250), 15 600 (sh) (500)	22 800, 18 000, 15 000 (sh)
$[Co_2L^2(NCS)_2(MeCN)_2][ClO_4]_2\cdot 2H_2O$	Orange-brown	4.70	4.13	2.01	2.20	81.5	22 700 (750), 19 200 (300), 14 800 (40)	
$[Co_2L^1(NCS)_2(MeCN)_2][BPh_4]_2$	Dark brown	3.54	2.13	2.25[d]	2.03[d]	96[d]	21 700 (2 500), 19 000 (2 300), 14 700 (sh)	
$[Co_2L^2(NCS)_2(MeCN)_2][BPh_4]_2$	Light brown	4.96	4.32	$g_\parallel > g_\perp$ complex spectrum			23 800 (800), 18 900 (500), 14 900 (230)	14 900
$[Cu_2L^1(NCS)_2][ClO_4]_2\cdot H_2O$	Blue-green	1.92	1.77	2.09	2.31	76	15 000 (290)	16 800 (sh), 14 500
$[Cu_2L^2(NCS)_2][ClO_4]_2\cdot 2H_2O$	Green	1.82	1.75	2.11	2.26	160[e]	14 600 (460), 12 000 (sh)	15 000
$[Cu_2L^1(NCS)_2][BPh_4]_2\cdot H_2O$	Green	1.94	1.81	2.09[d]	2.32[d]	78[d]	15 000 (360)	
$[Cu_2L^2(NCS)_2][BPh_4]_2$	Green	1.75	1.82	2.09[f]		160[e]	14 500 (390), 12 000 (sh)	
$PbMnL^1(NCS)_4$	Orange	5.7		2.02[f]		94		26 000 (sh)
$[PbFeL^1(NCS)_2(MeCN)_2][ClO_4]_2$	Dark purple	3.02	1.22				20 800 (4 500), 16 500 (sh)	20 800, 16 000
$[PbNiL^1(NCS)_2(MeCN)_2][ClO_4]_2$	Pale green	3.38						18 600, 11 700
$[Cu_2L^1(H_2O)_4][ClO_4]_4$	Blue	2.11	1.90	2.09	2.30	76	15 600 (250)	15 000
				$D^g = 140$ G				
$[Cu_2L^2(dmf)_2(H_2O)_2][ClO_4]_4$	Blue	1.96	1.96	2.08	2.28	140	15 500 (295)	

[a] Dmf glass unless otherwise specified. [b] ν/cm^{-1} (ε/dm^3 mol^{-1} cm^{-1}). [c] MeCN glass. [d] Polycrystalline spectrum. [e] Second derivative spectrum. [f] g_{iso}. [g] Zero-field splitting.

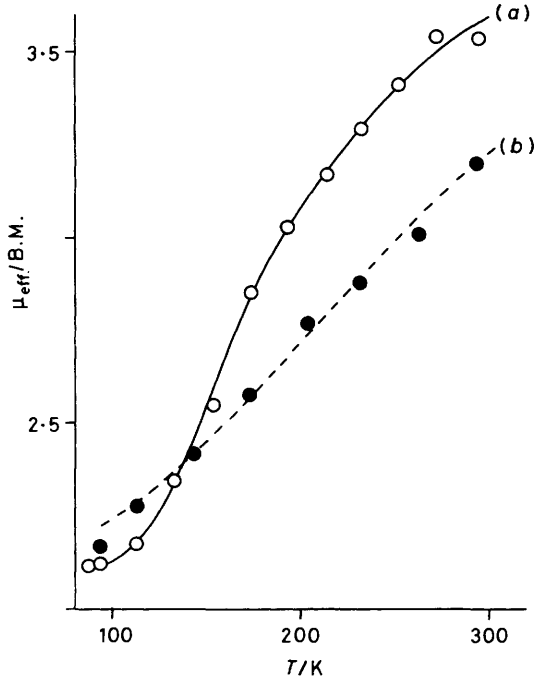

Figure 2. Temperature variation for $\mu_{eff.}$ for $[Co_2L^1(NCS)_2(MeCN)_2]X_2$ [X = BPh_4^- (*a*) or ClO_4^- (*b*)]

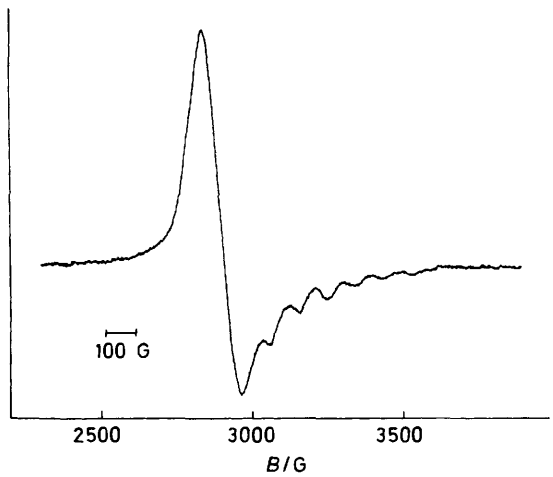

Figure 3. E.s.r. spectrum of $[Co_2L^1(NCS)_2(MeCN)_2][ClO_4]_2$ as MeCN glass

glass (Figure 3) in acetonitrile or dimethylformamide (dmf), but there was no indication of splitting of the eight hyperfine components into fifteen as might be expected if the two cobalt ions were interacting strongly.[5] In both polycrystalline and glass spectra, $g_\perp > g_\parallel$ indicating axially extended tetragonal geometry.[6] Polycrystalline $[Co_2L^2(NCS)_2(MeCN)_2][BPh_4]_2$ shows, even at 89 K, a broad, complex e.s.r. spectrum corresponding mainly to high-spin Co^{II}. However, from the appearance of hyperfine (and superhyperfine) structure on the low-field side of $g = 2$, it seems that for the low-spin form (present in a small amount at 89 K), $g_\parallel > g_\perp$ and the geometry is axially compressed tetragonal. This inference is reinforced by frozen solution spectra, because, although a frozen solution of

Table 3. Force field parameters[a]

(*a*) Bond stretching

Bond	k_s/mdyn Å^{-1}	r_o/Å
Co–S	1.00	2.65
Co–N	1.00	2.05
S–C	3.21	1.70

(*b*) Angle bending

Angle	k_b/mdyn Å^{-1} rad^{-2}	θ_o/°
Co–N–C (macrocycle)	0.550	121.13
Co–N–C (thiocyanate)	0.450	180.00
Co–S–C (thiocyanate)	0.500	90.00
S–C–N	1.500	180.00
N–Co–N	0.030	72.00, 144.00 (within macrocycle)
N–Co–N	0.030	90.00, 180.00
N–Co–S	0.030	90.00, 180.00

(*c*) Torsional terms

Force constants for angles including Co were set to zero

(*d*) Non-bonded parameters

Atom	r^*/Å	ε/kcal mol^{-1}
Co	2.35	0.165

[a] Nomenclature from ref. 7. Parameters not listed here are included within the MM2 program.

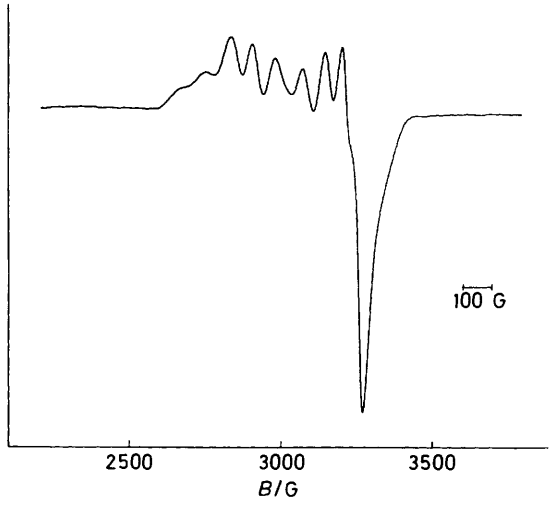

Figure 4. E.s.r. spectrum of $[Co_2L^2(NCS)_2(MeCN)_2][ClO_4]_2$ as dmf glass

$[Co_2L^2(NCS)_2]^{2+}$ in MeCN is of the high-spin type, a low-spin spectrum is obtained when dmf is used as solvent. This consists (Figure 4) of a simple signal with $g_{\|} > g_{\perp}$ and eight well resolved hyperfine lines in the parallel signal. Clearly the low-spin form is favoured in this strongly co-ordinating solvent.

It seems curious that, first, axial bonds should be longer in the 24-membered macrocyclic complex than in the 26-membered one, and secondly that the complex with axially compressed tetragonal geometry should be the one with a high-spin ground state.

In an attempt to rationalise these observations (and as crystals suitable for structure determination were not obtained), molecular mechanics calculations were performed on

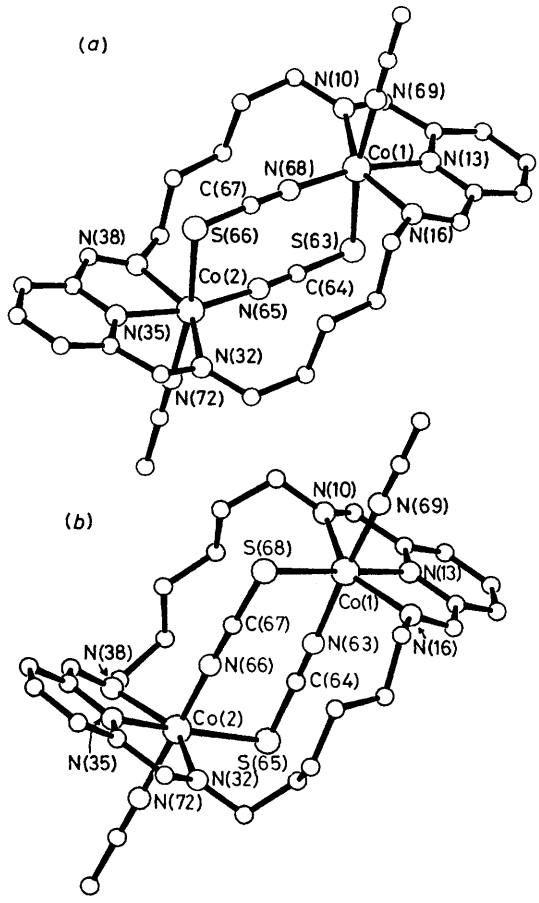

Figure 5. Structure of (*a*) $[Co_2L^1(NCS)_2(MeCN)_2]^{2+}$ and (*b*) $[Co_2L^2(NCS)_2(MeCN)_2]^{2+}$ as determined by molecular mechanics calculations

$[Co_2L(NCS)_2(MeCN)_2]^{2+}$ (L = L^1 or L^2) structures. There are two possible centrosymmetric arrangements, A and B, for the thiocyanate bridges in these complexes with the S-donor ends in either axial (A) or equatorial (B) positions (Figure 1). The molecular mechanics calculations were carried out using the MM2 program[7] in the manner described in ref. 8. Parameters were taken from ref. 7 except for those pertaining to thiocyanate bridges and the octahedral metal co-ordination spheres, which are listed in Table 3.

For $[Co_2L^1(NCS)_2(MeCN)_2]^{2+}$, the S-axial structure refined to a steric energy of 15.16 kcal mol^{-1} with a Co • • • Co distance of 5.43 Å, while the S-equatorial structure refined to a steric energy of 18.46 kcal mol^{-1} with a Co • • • Co distance of 5.72 Å. (Details of the refined structures are given in Table 4.) Some of the Co–N bond lengths obtained in the S-equatorial structure are unusually long [*e.g.* Co(1)–N(10) 2.34, Co(2)–N(38) 2.44 Å] despite an ideal Co–N bond length of 2.05 Å being included in the program. This clearly indicates instability in the structure. We increased the Co–N k_s force constant to 3.0 mdyn Å^{-1} and then the Co–N bond lengths refined to 2.05 Å but the steric energy increased to 20.5 kcal mol^{-1}, indicating that with the likely Co–N bond lengths of 2.05 Å, the S-equatorial structure would be severely strained. In $[Co_2L^1(NCS)_2(MeCN)_2]^{2+}$, the linking macrocyclic $-CH_2-$ groups are necessarily coplanar in order to accommodate the pair of thiocyanate bridges between the metal centres in the macrocycle. This is not the case in the L^2 complex, for which we found a suitable conformation with torsion angles around the –C–C– bonds of −135, 170, −51,

Table 4. Details of molecular mechanics calculations. Structure (I) $[Co_2L^1(NCS)_2(MeCN)_2]^{2+}$ with S-axial bridges, structure (II) $[Co_2L^1(NCS)_2(MeCN)_2]^{2+}$ with S-equatorial bridges, structure (III) $[Co_2L^2(NCS)_2(MeCN)_2]^{2+}$ with S-axial bridges, structure (IV) $[Co_2L^2(NCS)_2(MeCN)_2]^{2+}$ with S-equatorial bridges. [In (I) and (III), X = S, Y = N; in (II) and (IV) X = N, Y = S.] Dimensions in Å, angles in degrees

	(I)	(II)	(III)	(IV)		(I)	(II)	(III)	(IV)
Co(1)–N(10)	2.16	2.34	2.14	2.16	Co(2)–N(32)	2.17	2.08	2.16	2.16
Co(1)–N(13)	2.03	2.09	2.02	2.05	Co(2)–N(35)	2.03	2.10	2.03	2.05
Co(1)–N(16)	2.18	2.30	2.16	2.17	Co(2)–N(38)	2.17	2.44	2.17	2.17
Co(1)–X(63)	2.67	2.09	2.69	2.05	Co(2)–Y(65)	2.04	2.69	2.05	2.69
Co(1)–Y(68)	2.04	2.70	2.04	2.69	Co(2)–X(66)	2.69	2.10	2.68	2.05
Co(1)–N(69)	2.04	2.10	2.04	2.03	Co(2)–N(72)	2.04	2.10	2.04	2.03
N(10)–Co(1)–N(13)	75.2	71.9	74.6	74.0	N(32)–Co(2)–N(35)	74.8	75.5	74.9	74.2
N(10)–Co(1)–N(16)	149.2	144.1	143.3	145.5	N(32)–Co(2)–N(38)	149.8	146.1	144.4	145.5
N(10)–Co(1)–X(63)	88.9	79.2	93.8	91.6	N(32)–Co(2)–X(65)	93.5	103.8	108.1	109.3
N(10)–Co(1)–Y(68)	94.4	99.7	101.5	103.0	N(32)–Co(2)–Y(66)	91.1	88.6	99.7	85.6
N(10)–Co(1)–N(69)	91.4	95.9	79.3	85.5	N(32)–Co(2)–N(72)	89.9	94.6	80.8	82.7
N(13)–Co(1)–N(16)	75.2	73.1	74.4	73.7	N(35)–Co(2)–N(38)	75.9	70.6	74.0	73.7
N(13)–Co(1)–X(63)	78.5	92.0	78.8	90.8	N(35)–Co(2)–X(65)	167.1	176.6	165.1	175.1
N(13)–Co(1)–Y(68)	168.0	171.1	168.5	176.6	N(35)–Co(2)–Y(66)	79.5	93.5	73.9	85.6
N(13)–Co(1)–N(69)	87.4	85.0	86.7	86.7	N(35)–Co(2)–N(72)	86.7	84.7	88.8	89.1
N(16)–Co(1)–X(63)	93.7	93.9	99.0	100.8	N(38)–Co(2)–X(65)	116.4	110.1	106.4	103.6
N(16)–Co(1)–Y(68)	115.9	115.6	112.4	108.8	N(38)–Co(2)–Y(66)	90.8	92.4	87.9	90.1
N(16)–Co(1)–N(69)	78.6	89.2	79.8	80.7	N(38)–Co(2)–N(72)	81.1	83.4	81.6	84.5
X(63)–Co(1)–Y(68)	95.6	89.0	90.7	90.7	X(65)–Co(2)–Y(66)	95.6	89.8	91.2	90.4
X(63)–Co(1)–N(69)	165.3	174.9	165.2	176.6	X(65)–Co(2)–N(72)	98.9	92.0	106.2	94.6
Y(68)–Co(1)–N(69)	99.0	93.3	103.4	91.6	Y(66)–Co(2)–N(72)	165.4	175.7	161.6	173.4

Energy totals (kcal mol^{-1}) at the minimum energy conformation

	(I)	(II)	(III)	(IV)		(I)	(II)	(III)	(IV)
Compression	5.09	9.43	4.50	4.72	Torsional	4.53	5.23	5.10	6.20
Bending	15.19	12.14	16.16	12.17	Dipole	−9.59	−9.11	−11.58	−10.41
Stretch-bend	0.49	−0.32	0.38	0.32	Total	15.16	18.46	13.21	11.87
Van der Waals: 1,4	12.27	12.89	14.42	14.36					
:other	−12.82	−11.80	−15.77	−15.49					

−142, and 75.5°. For $[Co_2L^2(NCS)_2(MeCN)_2]^{2+}$, the centrosymmetric S-axial structure refined to a steric energy, at 13.21 kcal mol^{-1}, appreciably higher than that (11.87 kcal mol^{-1}) obtained for the S-equatorial structure. The Co ··· Co distances in both structures are similar (5.61 and 5.52 Å respectively). Details of the geometry of the refined structures are given in Table 4, and the proposed structure, with S-equatorial, is shown in Figure 5.

A search of the Cambridge Data Centre files showed 20 or so structures of transition metals with this type of di-1,3-μ-thiocyanate bridging. (No examples included cobalt.) The metal ··· metal distances ranged from 5.3 to 5.8 Å which fits in with the structures proposed here. It is interesting that the Pb ··· Mn distance in the $PbMnL^1(NCS)_4$ structure presented later is much lower, at 4.857(2) Å. This is due to the non-centrosymmetric nature of the bridge (lead is bonded to both sulphur atoms, manganese to both nitrogen atoms of the bridging thiocyanate), which permits the metal atoms to come closer to each other.

Our molecular mechanics calculations indicate that an S-axial arrangement is the preferred structure for $[Co_2L^1(NCS)_2(MeCN)_2]^{2+}$ but S-equatorial is preferred for the L^2 analogue. This accounts nicely for the e.s.r. spectra observed. Such a disposition of donors will of course lead in the first case to an axially extended and in the second an axially compressed tetragonal distortion. The explanation of why $[Co_2L^1(NCS)_2(MeCN)_2]^{2+}$ has a low-spin ground state, when $[Co_2L^2(NCS)_2(MeCN)_2]^{2+}$ does not, is less immediately obvious. However, the molecular mechanics calculations do indicate a high strain energy for the L^1 complex. This strain would presumably be relieved on formation of the smaller low-spin Co^{II} ion, thus providing a thermodynamic driving force for the $^4T_{1g} \rightarrow {}^2E_g$ transition.

Room-temperature electronic spectra of the dicobalt(II) complexes of L^1 and L^2 in acetonitrile are similar; each shows three bands at very similar frequencies which correspond to transitions from the $^4T_{1g}$ ground state of octahedral Co^{II} to $^4T_{2g}$, $^4A_{2g}$, and $^4T_{1g}(P)$ excited states. Much higher intensities are observed in the L^1 complex, which is at least partly due to overlapping with the more intense metal-to-ligand charge transfer (m.l.c.t.) absorption originating in the low-spin form, present in a significant proportion at ambient temperature.

Dicopper(II) Complexes.—For the dicopper(II) complexes of L^1, variable-temperature magnetic susceptibility data indicate a weak antiferromagnetic interaction. E.s.r. spectra also suggest weak exchange between the copper centres. Hyperfine splitting in the $\Delta m = 1$ signal of these compounds (Figure 6) is more complex than can be explained on the basis of independent Cu^{II} ions, five or six components being clearly resolved in the parallel band before it becomes obscured by the perpendicular signal. (However, no zero-field splitting was resolved in the perpendicular signal.) The forbidden 'half-band', $\Delta m = 2$, signal is also observable in the polycrystalline $[Cu_2L^1(NCS)_2][BPh_4]_2$ sample.

The spectrum of $[Cu_2L^1(H_2O)_4][ClO_4]_4$, run as dmf glass (Figure 7), is not a simple axial-type spectrum. The two strong features around $g = 2$ may arise because of rhombic distortion, or as a consequence of zero-field splitting which generates a triplet-type spectrum. While the complex hyperfine pattern

Table 5. Fast-atom bombardment mass spectra[a]

	$[PbML(NCS)_2(ClO_4)]^+$		$[PbML(NCS)_2]^{\cdot+}$		$[ML]^{\cdot+}$	
Complex	*M/z*	R.i.	*M/z*	R.i.	*M/z*	R.i.
$[PbFeL^1(NCS)_2(MeCN)_2][ClO_4]_2$	937	30	838	40	513	100
$[PbNiL^1(NCS)_2(MeCN)_2][ClO_4]_2$	939	90	841	42	516	100
$[PbMnL^1(NCS)_2][ClO_4]_2$[b]	936	28	837	50	512	100

[a] Positive-ion mode using 3-nitrobenzyl alcohol matrix; r.i. = relative intensity. [b] Impurity peak at *m/z* 1 089 corresponding to $[Pb_2L^1(NCS)_2][ClO_4]^+$ (at 12% intensity of 936 peak).

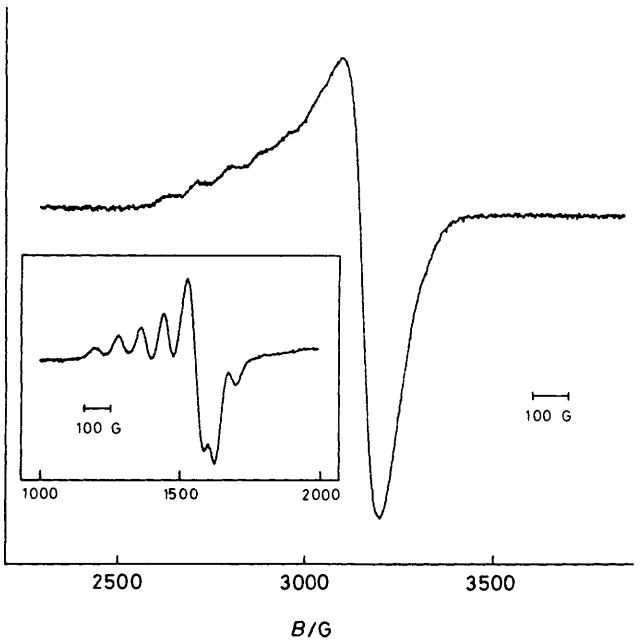

Figure 6. E.s.r. spectrum of $[Cu_2L^1(NCS)_2][BPh_4]_2$ as dmf glass

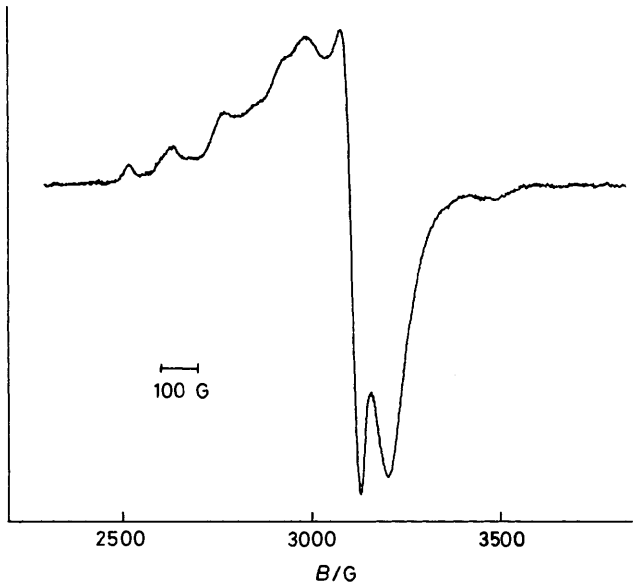

Figure 7. E.s.r. spectrum of $[Cu_2L^1(H_2O)_4][ClO_4]_4$ as dmf glass

favours the latter explanation, the variable-temperature magnetic susceptibility data do not suggest any strong exchange interaction. However, with a zero-field splitting of only *ca.* 140 G, such a magnetic interaction might not be easily observable in the temperature range available. The weak interaction observed in dicopper(II) complexes of ligand L^1 is qualitatively similar to that seen [9] in dicopper(II) complexes of related ligands with 5—7 Å between the metal centres. The distance between copper ions in L^1 complexes lies in the 5—6 Å range. When azide ion acts as a symmetrically disposed 1,3-bridge between copper ions, it can mediate sizeable antiferromagnetic coupling.[10] (However, 1,3-bridging azide does not always give rise to strong exchange interaction as shown by our earlier studies on related macrocycles.[11]) The present results suggest that the 1,3-μ-thiocyanato –NCS– bridge is not a good transmitter of magnetic exchange interactions.

In the 26-membered macrocycle L^2, there is virtually no indication of interaction between the copper(II) centres. Thus, the tetraperchlorate, $[Cu_2L^2(dmf)_2(H_2O)_2][ClO_4]_4$ shows almost perfect Curie-law magnetic behaviour with a temperature-independent moment of 1.96 B.M., and its e.s.r. spectrum displays a poorly resolved four-line pattern in the $g_{\|}$ signal with a coupling constant of *ca.* 140 G, indicative of non-interacting copper centres. The bis-thiocyanato derivative of this complex, $[Cu_2L^2(NCS)_2][ClO_4]_2 \cdot 2H_2O$, examined as a glass in dmf, likewise shows a poorly resolved four-line hyperfine pattern with $A_{\|}$ *ca.* 160 G. In the broad signal obtained from polycrystalline $[Cu_2L^2(NCS)_2][BPh_4]_2$ a very poorly resolved hyperfine splitting of *ca.* 160 G is just discernible in the 93 K spectrum on the low field side of $g = 2.1$. The breadth of signal observed in both glass and polycrystalline samples of dicopper(II) complexes of this ligand suggests [12] that a dynamic Jahn-Teller effect may be in operation.

Heterobinuclear Complexes of L^1.—Transmetallation of $Pb_2L^1(NCS)_4$ with excess Ni^{II} or Fe^{II} results in the isolation of crystalline solids analysing to the formula $PbML^1(NCS)_2(ClO_4)_2 \cdot 2MeCN$ (M = Ni or Fe). When $Pb_2L^1(ClO_4)_4$ was treated with excess $Mn(NCS)_2$ the compound $PbMnL^1(NCS)_4$ was isolated. Fast-atom bombardment (f.a.b.) mass spectra (Figure 8 and Table 5) confirm the existence of the heterobinuclear ions $[PbNiL^1(NCS)_2(ClO_4)]^+$ and $[PbFeL^1(NCS)_2(ClO_4)]^+$, while an *X*-ray crystallographic structure determination confirmed the formulation of the lead–manganese compound.

The bis-thiocyanato heterobinuclear complexes were in general too insoluble for satisfactory measurements of solution properties, so co-ordination geometry has to be inferred from solid-state measurements. I.r. spectra indicate that NCS^- is co-ordinated in a 1,3-μ –NCS– bridging mode; $\nu_{asym}(NCS)$ is centred about 2 100 cm^{-1} in both complexes. I.r. spectra reveal acetonitrile to be co-ordinated, showing that both metal ions are six-co-ordinate. In the absence of crystallographic data it is not possible to say whether the thiocyanate bridges present both S-donors to lead and both N-donors to the transition-metal ion,

as happens in $PbMnL^1(NCS)_4$. However, whatever the arrangement of NCS groups, it is clearly one of low symmetry as the splitting of $\nu_{asym}(NCS)$ into three components demonstrates. The low symmetry of these complexes is also demonstrated by the splitting of the macrocyclic $\nu(C{=}N)$ imino absorption into two components, one at the frequency typical of C=N co-ordinated to lead and the other, 10—15 cm^{-1} lower, at the frequency typical of C=N co-ordinated to transition metals.

Six-co-ordination is confirmed for Ni^{II} in $[PbNiL^1(NCS)_2(MeCN)_2]^{2+}$ by electronic spectral and magnetic susceptibility measurements (Table 2). Thus absorption bands are seen at 18 600 and 11 700 cm^{-1}, attributable to two out of the three transitions expected for Ni^{II} in an octahedral symmetry. The highest energy $^3A_{2g} \rightarrow {}^3T_{1g}(P)$ transition is unobservable because of intense ligand absorption above 24 000 cm^{-1}. The room-temperature magnetic moment is as expected for octahedral Ni^{II}.

Room-temperature magnetic susceptibility measurements for $[PbFeL^1(NCS)_2(MeCN)_2][ClO_4]_2$ however, reveal a moment (at 3.02 B.M.) intermediate between the value expected for ^5E and ^1A ground states, suggesting the existence of a thermally populated spin equilibrium. At 93 K, the complex is close to diamagnetic, showing that the equilibrium lies almost completely to the low-spin side at this temperature. The change in magnetic moment with temperature is gradual,[13] continuous over the 200 °C range studied. The intense colour of the complex, and its electronic absorption spectrum, consisting of an intense charge-transfer absorption centred around 20 000 cm^{-1}, confirm that Fe^{II} is mainly in the low-spin state at room temperature. The charge-transfer absorption includes a low-frequency shoulder indicative[14] of some degree of distortion from octahedral symmetry.

The properties of $PbMnL^1(NCS)_4$ are in accord with the structure determined by *X*-ray diffraction. Thus, the magnetic moment is as expected for an isolated Mn^{II} ion, and no absorptions corresponding to *d–d* transitions are observed in the electronic absorption spectrum. The e.s.r. spectrum consists of a strong isotropic signal at $g \approx 2$ split into six lines by hyperfine coupling of 94 G. 'Forbidden' lines due to quadrupole interactions appear weakly between the allowed hyperfine-split lines, as normally observed in Mn^{II} spectra.

Presumably owing to the high insolubility of this compound, f.a.b. spectra were not observed. The i.r. spectrum contains three $\nu_{asym}(NCS)$ absorptions, that at 2 022 cm^{-1} most likely corresponding to terminal Pb(NCS) and those at 2 062 cm^{-1} and 2 090 cm^{-1} to terminal Mn(NCS) and bridging Mn–NCS–Pb respectively. An attempt was made to prepare the bis-thiocyanato complex $[PbMnL^1(NCS)_2][ClO_4]_2$ in order to obtain a f.a.b. spectrum of the heterobinuclear ion. This was obtained, as shown in Figure 8, but the sample was impure, containing 10—15% of the dilead complex $[Pb_2L^1(NCS)_2][ClO_4]_2$ as shown by analytical data and the relative intensity of the $[M_2L^1(NCS)_2(ClO_4)]^+$ peaks. A strong low-frequency i.r. $\nu_{asym}(NCS)$ absorption at 1 965 cm^{-1} seemed too intense to result from 15% dilead impurity, which raises the possibility that a short N(CS) bridge may exist in $[PbMnL^1(NCS)_2][ClO_4]_2$ between lead and the largest of the M^{2+} ions.

Structure of $PbMnL^1(NCS)_4$.—The geometry of the proposed ordered molecule of $PbMnL^1(NCS)_4$ is shown in Figure 9 together with the atomic numbering scheme. The positions of the Pb and Mn atoms are related by a centre of symmetry, with a separation of 4.857(2) Å. Each metal is six-co-ordinate being bonded to three nitrogen atoms of the macrocycle, a nitrogen atom of a terminal NCS group, and two atoms of the bridging thiocyanate groups. In an ordered model we would expect the Pb atom to be bonded to both sulphur atoms and the Mn atom to both nitrogen atoms, and this is shown in Figure 9. The evidence for this is based on data located

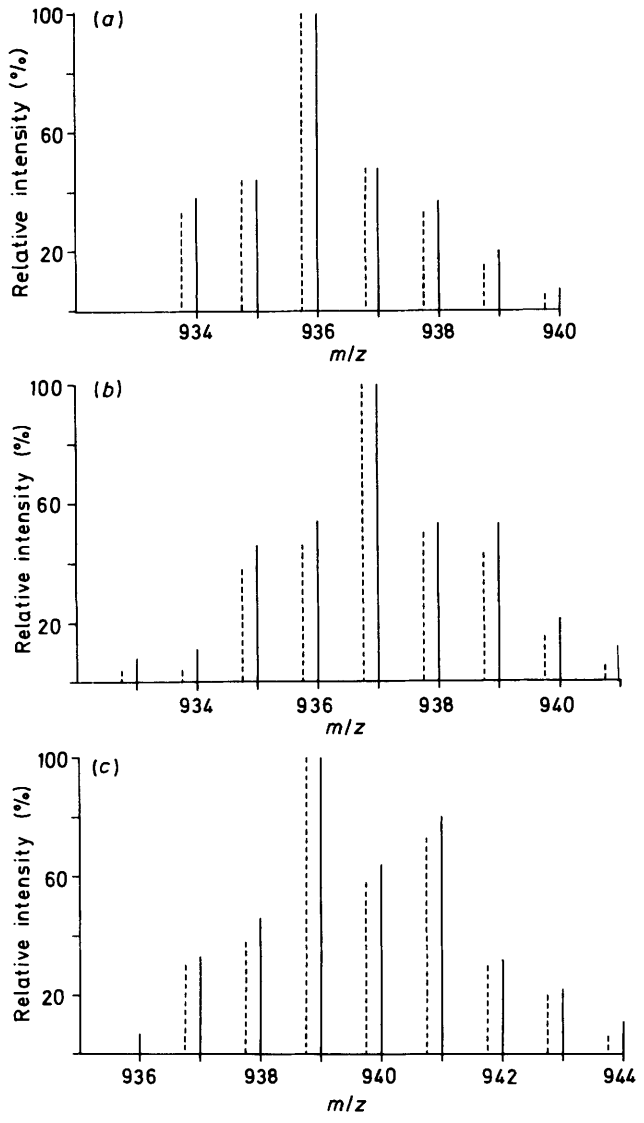

Figure 8. F.a.b. mass spectra of the $[PbML^1(NCS)_2(ClO_4)]^+$ isotopic cluster. Comparison of observed (——) and calculated (– – – –) intensities. (*a*) M = Mn; (*b*) M = Fe; (*c*) M = Ni

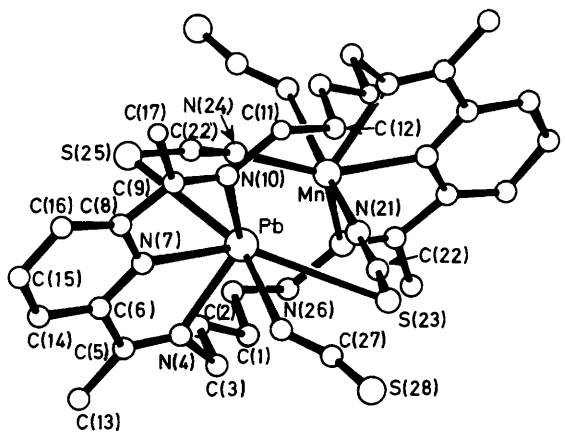

Figure 9. The crystal structure of $PbMnL^1(NCS)_4$

in the Cambridge Data Centre files. We searched for all structures containing Pb or Mn bonded to a thiocyanate ligand. There were only about 10 structures with each metal, though the type of bonding falls into a distinct pattern. In manganese structures the thiocyanate ligands are almost always bonded to the metal through nitrogen, with bond lengths ranging from 2.1 to 2.3 Å. There is only one example of a thiocyanate bonded through sulphur, with a distance of 2.69 Å.[14] In lead structures the ligand is usually bonded to the metal *via* sulphur with bond lengths in the range 2.8—3.2 Å. There is just one example of an N-bonded thiocyanate with a Pb–N distance of 2.42 Å.[15] This structural information strongly suggests that in the present structure lead will be bonded through sulphur and manganese through nitrogen and the observed bond lengths [*viz.* M–N 1.92(5), 2.16(5), and M–S 3.26(2), 3.34(2) Å] confirm this assignment.

The Pb • • • Mn distance is 4.857(2) Å. This distance is much shorter than all known metal • • • metal distances in centrosymmetric di-1,3-μ-thiocyanate bridges (range 5.3—5.8 Å[16]) and indeed the Co • • • Co distances calculated *via* molecular mechanics for this macrocycle in $[Co_2L^1(NCS)_2(MeCN)_2]^{2+}$. Such evidence also strongly suggests that the structure does not contain a centrosymmetric bridge.

It would seem likely that these strong preferences for Pb–S and Mn–N bonds have prevented formation of an ordered structure in space group $P\bar{1}$ in which each metal is bonded similarly to one sulphur and one nitrogen of the two bridging thiocyanates. The Pb/Mn–N bond lengths to the macrocycle are 2.43(2), 2.26(2), and 2.41(2) Å. Several structures have been determined in which the Pb or Mn is enclosed within this trimethine moiety in a macrocycle.[17–21] Bond lengths for Pb–N are 2.46—2.64 Å in ref. 19 and for Mn–N 2.21—2.25 Å in ref. 20. A difference of *ca.* 0.25 Å between these Pb–N and Mn–N distances is therefore to be expected. This difference is probably concentrated primarily in the nitrogen positions of the macrocycle. The Mn/Pb distance to the terminal N-bonded thiocyanate is 2.54(2) Å. While it would appear that there is some disorder in the position of this ligand because of the different size metal atoms, the electron density distribution is compatible with N-bonded thiocyanate rather than a mix of N- and S-bonded thiocyanate.

The effect of the disorder in the thiocyanate bridges has been to give different geometries for the co-ordination spheres of Mn and Pb. Thus for Mn the two nitrogen atoms complete a distorted octahedron with N(21) *trans* to N(26), 176.1(17), and N(24′) *trans* to the pyridine nitrogen N(7), 161.4(12)°. There is more distortion in the Pb co-ordination sphere with S(25)–Pb–N(26) 154.3(5) and S(23′)–Pb–N(7) 147.6(5)°. This distortion suggests that the lone pair on the lead may be stereochemically active but the disorder prevents determination of its likely position. The metal atoms are approximately coplanar with the trimethine unit of the macrocycle. The maximum deviation of an atom from the plane containing C(3), N(4), C(5), C(6), N(7), C(8), C(9), N(10), and C(11)—C(17) is only 0.15 Å. The metal atom is 0.14 Å from this plane. The torsion angles along the pentane linkage from C(5)–N(4)–C(3)–C(2) to C(12′)–C(11′)–N(10′)–C(9′) are −86.8, −162.7, −172.7, −169.7, 80.4, and 173.1°. Some of these values are considerably different from the 180 and 60° expected and may indicate some disorder or some steric effect induced by the two thiocyanate bridges and the necessity of accommodating a Pb • • • Mn distance of 4.857(2) Å. However the conformation of these linkages is equivalent to that found in $Pb_2L^1(NCS)_4$[1] despite the 0.51 Å increase in the metal • • • metal distance.

Conclusions

With the possible exception of $[PbMnL^1(NCS)_2][ClO_4]_2$, none of the transition-metal derivatives of these ligands shows the unusual single-atom >NCS bridge observed in their dilead analogues. It seems that the 1,3-μ –NCS– bridge may be accommodated between transition-metal centres in both 24- and 26-membered macrocycles and that it is the preferred mode of co-ordination. A smaller macrocyclic cavity, such as that in 22- or 20-membered macrocycles may be required to achieve >NCS bridging between transition-metal ions.

This work extends the range of bonding situations observed for thiocyanate in binuclear complexes of these relatively restricting macrocycles. In addition to the previously characterised[1] single-atom >NCS bridge, we now identify two forms of centrosymmetric axial–equatorial 1,3-μ –NCS– bridge and a non-centrosymmetric type with both nitrogens co-ordinated to one metal and both sulphurs to the other in a distorted axial–equatorial arrangement. This latter bridge permits closer approach of the metal centres than has been observed to date in 1,3-μ –NCS– dinuclear complexes.

There are marked differences in the co-ordinating behaviour of the two N_6 macrocycles studied. Both act as binucleating ligands, but the 26-membered macrocycle co-ordinates two metal ions in such a way that they are virtually independent of each other, while weak interaction can be observed in Cu^{II} complexes of the smaller macrocycle. The ligand field around Co^{II} in the bis-thiocyanate complex of the smaller macrocycle is strong enough to ensure a low-spin ground state at 83 K [to our knowledge the first example of spin crossover in a dicobalt(II) complex], while in the analogous complex of the larger macrocycle, Co^{II} remains essentially high-spin, down to 93 K.

It is not clear why transmetallation of $PbL^1(NCS)_4$ with Mn^{II} or Ni^{II} should result in the formation of heterobimetallic complexes. While this may be a solubility effect unrelated to any structural considerations, it is noticeable that the transition metals involved do not often form homobinuclear complexes in macrocycles of this type. The size of the macrocyclic cavity may be insufficient to contain the longer centrosymmetric bridge which requires 5.3—5.8 Å between the metal centres but adequate to the steric requirements of a non-centrosymmetric bridge of the Pb–Mn type described above. Or it may be that owing to steric constraints, the site geometry is unsuitable for binuclear Mn^{II}, Fe^{II}, or Ni^{II} complexes, while the less sterically demanding Pb^{II} ion can accommodate the irregular geometry offered by the second co-ordination site. If this is so, it offers the interesting possibility of replacing the Pb^{II} ion by a sterically accommodating transition-metal ion to produce heterobinuclear transition metal complexes.

Experimental

Preparation of the Complexes.—$[Cu_2L^1(NCS)_2][ClO_4]_2 \cdot H_2O$. $Pb_2L^1(NCS)_4$ (0.001 mol) and $Cu(ClO_4)_2 \cdot 6H_2O$ (0.002 mol) were stirred together at 60 °C for 30 min in acetonitrile (50 cm^3). After filtering off the white precipitate, EtOH (50 cm^3) was added to the filtrate and the volume was reduced by 50% on a rotary evaporator. Small blue-green crystals of product were obtained on standing.

$[Cu_2L^2(NCS)_2][ClO_4]_2 \cdot 2H_2O$. Preparation was analogous to that above, using a 50:50 dmf–EtOH solvent.

$[Co_2L(NCS)_2(MeCN)_2][ClO_4]_2 \cdot 2H_2O$, L = L^1 *or* L^2. $Pb_2L(NCS)_4$ (0.001 mol) and $Co(ClO_4)_2 \cdot 6H_2O$ (0.002 mol) were stirred together at 60 °C for 30 min in acetonitrile (200—300 cm^3). After filtering, the brown solution was reduced in volume by about half, and allowed to crystallise. The complexes could be obtained as tetraphenylborate salts by adding excess sodium tetraphenylborate to a solution of the perchlorate salt in acetonitrile, and allowing it to crystallise slowly in the presence of ethanol.

$[Cu_2L^1(H_2O)_4][ClO_4]_4$. $[Pb_2L^1][ClO_4]_4$ (0.005 mol), pre-

pared as described elsewhere,[1] was mixed with $Cu(ClO_4)_2 \cdot 6H_2O$ (0.001 mol) in acetonitrile (100 cm^3). Ethanol (20 cm^3) was added, the volume reduced by about half, and the solution left to crystallise as royal blue cubes.

$[Cu_2L^2(dmf)_2(H_2O)_2][ClO_4]_4$. Preparation was analogous to that above except that dmf (5 cm^3) was added to the acetonitrile–ethanol solvent.

$PbMnL^1(NCS)_4$. $[Pb_2L^1][ClO_4]_4$ (0.000 25 mol) and $Mn(ClO_4)_2 \cdot 6H_2O$ (0.0005 mol) were dissolved in dry acetonitrile (100 cm^3). Excess Li(NCS) (0.01 mol) was added, and the clear yellow solution left after filtering off $Pb(NCS)_2$ was slowly evaporated to yield orange crystals.

$[PbMnL^1(NCS)_2][ClO_4]_2$. $[Pb_2L^1][ClO_4]_4$ (0.000 25 mol) and $Mn(ClO_4)_2 \cdot 6H_2O$ (0.0005 mol) were mixed in dry acetonitrile (100 cm^3). Li(NCS) (0.001 mol) was added and the solution filtered. The filtrate was concentrated by a factor of 3, whereupon the yellow solid crystallised out.

$[PbFeL^1(NCS)_2(MeCN)_2][ClO_4]_2$. $Pb_2L^1(NCS)_4$ (0.001 mol) and $Fe(ClO_4)_2 \cdot 6H_2O$ (0.001 mol) were stirred together in dry deoxygenated acetonitrile (120 cm^3) under N_2. After filtering, the deep wine coloured filtrate was reduced in volume to 30 cm^3 by bubbling through N_2 in the warm (50—60 °C), then filtered under N_2 into an equal volume of deoxygenated ethanol. Dark purple crystals separated out on further evaporation.

$[PbNiL^1(NCS)_2(MeCN)_2][ClO_4]_2$. $Pb_2L^1(NCS)_4$ (0.0005 mol) and $Ni(ClO_4)_2 \cdot 6H_2O$ (0.001 mol) were stirred together for 30 min in warm acetonitrile (80 cm^3). After filtering off the beige precipitate, the filtrate was evaporated slowly to yield khaki-green crystals.

X-Ray Crystallography.—Crystal data. $PbMnL^1(NCS)_4$, $C_{32}H_{38}MnN_{10}PbS_4$, $M = 953.1$, triclinic, $a = 8.18(1)$, $b = 13.02(1)$, $c = 10.04(1)$ Å, $\alpha = 111.1(1)$, $\beta = 80.4(1)$, $\gamma = 83.1(1)°$, $U = 966.0$ Å^3, $D_m = 1.62(3)$ g cm^{-3}, $D_c = 1.64$ g cm^{-3}, $Z = 1$, $F(000) = 471$, Mo-K_α radiation, $\lambda = 0.7107$ Å, $\mu = 49.5$ cm^{-1}, space group $P\bar{1}$ from the successful structure determination.

A crystal of approximate size 0.70 × 0.25 × 0.10 mm was mounted on a Stoe Stadi-2 diffractometer and data collected *via* variable width ω scan. Background counts were 20 s and the scan rate of 0.033° s^{-1} was applied to a width of (2.0 + sinμ/tanθ). 2 809 Independent reflections with $2\theta < 50°$ of which 1 685 with $I > 3\sigma(I)$ were used in subsequent refinement. An empirical absorption correction was applied. A disordered structure was refined in space group $P\bar{1}$. The position of the metal atom was obtained from the Patterson function and given a scattering factor of $\frac{1}{2}(f_{Pb} + f_{Mn})$. The positions of the macrocycle atoms were located and found to be consistent with space group $P\bar{1}$. The bridging thiocyanate ligands were not compatible with the centre of symmetry and two distinct NCS groups were refined, each with 0.5 occupancy. The carbon atom C(22) was common to both bridging groups.

From a calculation of the distances between the thiocyanates over the centre of symmetry it emerges that there is only one possible arrangement for the bridges, namely one in which the two sulphur atoms are bonded to one metal and the two nitrogens bonded to the other. There is much evidence (see Results and Discussion section) to suggest that the lead atom is bonded to the sulphur atoms and manganese to the nitrogen atoms. Attempts to refine an ordered molecule in space group $P1$ were unsuccessful and so refinement proceeded in $P\bar{1}$ assuming the disordered model. Hydrogen atoms were included in calculated positions, with a common thermal parameter which was refined.

The expected Pb–N and Mn–N bond lengths should differ by *ca.* 0.25 Å and therefore some of the macrocycle atoms must be disordered over two positions approximately this distance apart. However we were unable to find a suitable way of treating this disorder and so macrocycle atoms were refined normally. Presumably any disorder was taken up by the anisotropic thermal parameters, although this was not apparent in their refined values. The thiocyanates proved more difficult to treat. In the bridge the sulphur atoms were refined anisotropically and the nitrogen atoms isotropically. Assuming normal geometry for the thiocyanate ligand, the two carbon atom positions were calculated to be 0.15 Å apart. We considered refining the two positions independently of each other but as part of rigid groups but decided the most appropriate treatment was to refine one carbon atom in an average position. The metal disorder clearly affected the position of the terminal thiocyanate ligand. However we decided to refine the atom positions (N and C isotropic, S anisotropic) independently without constraints. The

Table 6. Molecular dimensions in the co-ordination sphere of $PbMnL^1(NCS)_4$; distances in Å, angles in degrees

Pb/Mn–N(4)	2.431(19)	Pb/Mn–N(10)	2.411(21)
Pb/Mn–N(7)	2.264(20)	Pb/Mn–N(26)	2.544(25)
Pb–S(25)	3.340(21)	Mn–N(21)	1.92(5)
Pb–S(23′)	3.257(15)	Mn–N(24′)	2.16(5)
N(4)–Pb/Mn–N(7)	67.6(6)	N(10)–Pb–S(23′)	118.0(6)
N(4)–Pb/Mn–N(10)	135.9(6)	N(26)–Pb–S(23′)	68.3(5)
N(7)–Pb/Mn–N(10)	68.6(6)	S(25)–Pb–S(23′)	135.6(3)
N(4)–Pb/Mn–N(26)	84.8(8)	N(21)–Mn–N(4)	92.5(16)
N(7)–Pb/Mn–N(26)	81.6(7)	N(21)–Mn–N(7)	100.0(16)
N(10)–Pb/Mn–N(26)	84.5(8)	N(21)–Mn–N(10)	99.4(17)
N(4)–Pb–S(25)	82.7(6)	N(21)–Mn–N(26)	176.1(17)
N(7)–Pb–S(25)	72.8(6)	N(24′)–Mn–N(4)	97.9(14)
N(10)–Pb–S(25)	88.9(6)	N(24′)–Mn–N(7)	161.4(12)
N(26)–Pb–S(25)	154.3(5)	N(24′)–Mn–N(10)	123.6(16)
N(4)–Pb–S(23′)	97.0(6)	N(24′)–Mn–N(26)	85.5(14)
N(7)–Pb–S(23′)	147.6(5)	N(24′)–Mn–N(21)	92.2(20)

Symmetry element, prime indicates: $1 - x, -y, -z$.

Table 7. Atomic co-ordinates (× 10^4) with estimated standard deviations in parentheses

Atom	*x*	*y*	*z*
Pb/Mn	4 582(2)	1 893(1)	1 819(1)
C(1)	1 299(45)	−1 026(22)	799(28)
C(2)	1 821(33)	−253(24)	2 080(30)
C(3)	1 101(34)	1 003(24)	2 376(29)
N(4)	2 094(23)	1 678(16)	3 319(21)
C(5)	1 891(34)	2 062(16)	4 664(29)
C(6)	3 153(43)	2 703(18)	5 294(24)
N(7)	4 402(24)	2 806(15)	4 243(20)
C(8)	5 584(35)	3 402(19)	4 763(26)
C(9)	6 806(29)	3 476(15)	3 577(28)
N(10)	6 789(25)	2 964(12)	2 251(23)
C(11)	8 012(40)	3 065(21)	1 058(24)
C(12)	7 804(44)	2 241(20)	−397(24)
C(13)	502(35)	1 957(28)	5 748(29)
C(14)	3 061(37)	3 168(23)	6 722(30)
C(15)	4 235(62)	3 730(28)	7 131(33)
C(16)	5 666(34)	3 799(23)	6 180(24)
C(17)	8 289(21)	4 090(18)	4 015(31)
N(21)	5 808(63)	447(41)	1 525(52)
C(22)	6 517(32)	−599(22)	1 337(27)
S(23)	7 011(18)	−1 700(11)	1 008(14)
N(24)	6 114(59)	−1 245(39)	266(50)
S(25)	6 557(15)	85(12)	2 972(12)
N(26)	2 788(36)	3 745(20)	2 171(22)
C(27)	2 291(21)	4 171(14)	1 533(19)
S(28)	1 405(16)	5 013(10)	1 099(12)

resulting dimensions were somewhat unreasonable but as the refined positions were the average of two, this was not surprising.

Refinement was carried out by full-matrix least squares with a weighting scheme of $w = 1/[\sigma^2(F) + 0.003F^2]$. Scattering factors were taken from ref. 22. Calculations were performed using SHELX 76[23] on the Amdahl V7A computer at the University of Reading. The final R value was 0.081 ($R' = 0.085$). In the final cycles of refinement no shift was $>0.16\sigma$. In a final difference Fourier map the maximum and minimum peaks were at heights of 1.1 and -1.0 e Å^{-3}. Final co-ordinates are given in Table 6 and bond lengths and angles in the metal co-ordination spheres are given in Table 7. Additional material available from the Cambridge Crystallographic Data Centre comprises the H-atom co-ordinates, thermal parameters, and remaining bond lengths and angles.

Physical measurements were made as described in earlier papers.[1,9] F.a.b. mass spectra were obtained on a Kratos (MS80) spectrometer at Sheffield University.

Acknowledgements

We thank the Open University for a Higher Degrees Studentship (to B. P. M.), the S.E.R.C. for funds for the Varian E109 e.s.r. spectrometer, the λ9 ultraviolet spectrometer, the diffractometer, and for a studentship (to P. C. Y.). We acknowledge the assistance of Mr. A. Johans of the University of Reading in the crystallographic investigations, and of Ian Johnstone and Peter Ashton of Sheffield University in obtaining f.a.b. mass spectra.

References

1 B. P. Murphy, J. Nelson, M. G. B. Drew, P. Yates, and S. M. Nelson, *J. Chem. Soc., Dalton Trans.*, 1987, 123.
2 G. A. Van Albada, R. A. G. de Graaff, G. A. Haasnoot, and J. Reedjik, *Inorg. Chem.*, 1984, **23**, 1404 and refs. therein.
3 W. J. Geary, *Coord. Chem. Rev.*, 1971, **1**, 81.
4 W. Stratton and D. H. Busch, *J. Am. Chem. Soc.*, 1960, **82**, 4834.
5 E. A. V. Ebsworth and J. A. Weil, *J. Phys. Chem.*, 1959, **63**, 1890.
6 Y. Nishida, K. Ida, and S. Kida, *Inorg. Chim. Acta*, 1980, **38**, 113.
7 N. L. Allinger and Y. H. Yah, MM2 program, Q.C.P.E. Program No. 423, Quantum Chemistry Program Exchange, Indiana University Chemistry Department, Indiana, U.S.A. 1977, modified version 1980.
8 M. G. B. Drew and P. C. Yates, *J. Chem. Soc., Dalton Trans.*, 1987, 2563.
9 B. P. Murphy, J. Nelson, M. G. B. Drew, and S. M. Nelson, *J. Chem. Soc., Dalton Trans.*, 1987, 873; M. G. B. Drew, M. McCann, and S. M. Nelson, *J. Chem. Soc., Dalton Trans.*, 1981, 1869.
10 O. Kahn, S. Sikorav, J. Gouteron, S. Jeannin, and Y. Jeannin, *Inorg. Chem.*, 1983, **22**, 2877.
11 M. G. B. Drew, M. McCann, and S. M. Nelson, *J. Chem. Soc., Chem. Commun.*, 1979, 481.
12 G. F. Kososzka, C. W. Reiman, H. C. Allen, and G. Gordon, *Inorg. Chem.*, 1967, **6**, 1657.
13 E. Konig, G. Ritter, S. K. Kulshreshta, and S. M. Nelson, *J. Am. Chem. Soc.*, 1983, **105**, 1924.
14 S. M. Nelson, M. McCann, C. Stevenson, and M. G. B. Drew, *J. Chem. Soc., Dalton Trans.*, 1979, 1477.
15 J. N. McElearney, L. L. Balagot, J. A. Muir, and R. D. Spence, *Phys. Rev. B, Condens. Mat.*, 1979, **9**, 306.
16 J. de O. Cabral, M. F. Cabral, W. J. Cummins, M. G. B. Drew, A. Rodgers, and S. M. Nelson, *Inorg. Chim. Acta*, 1978, **30**, L313.
17 Cambridge Crystallographic Data Centre files, June 1986 update.
18 M. G. B. Drew, A. Rodgers, M. McCann, and S. M. Nelson, *J. Chem. Soc.*, 1978, 416.
19 M. G. B. Drew and S. M. Nelson, *Acta Crystallogr., Sect. B*, 1979, **35**, 1594.
20 M. G. B. Drew, A. H. bin Othman, S. G. McFall, P. D. A. McIlroy, and S. M. Nelson, *J. Chem. Soc., Dalton Trans.*, 1977, 438.
21 M. G. B. Drew, A. H. bin Othman, S. G. McFall, P. D. A. McIlroy, and S. M. Nelson, *J. Chem. Soc., Dalton Trans.*, 1977, 1173.
22 'International Tables for *X*-Ray Crystallography,' Kynoch Press, Birmingham, 1974, vol. 4.
23 G. M. Sheldrick, SHELX 76, Package for Crystal Structure Determination, University of Cambridge, 1976.

Received 10*th February* 1987; *Paper* 7/242